Received February 1998
Revised October 1998
Accepted January 1999

Interaction of surface radiation and variable property natural convection in a differentially heated square cavity – a finite element analysis

S.K. Mahapatra, S. Sen and A. Sarkar
Application Software R&D Laboratory, Department of Mechanical Engineering, Jadavpur University, Calcutta, India

Keywords *Finite element method, Laminar flow, Natural convection*

Abstract *A finite element solution on the interaction of surface radiation and variable property laminar natural convection is presented. Finite element formulation of the governing equations, associated with variable property natural convection, and incorporation of the radiative boundary conditions has been extensively discussed. The study also aims to highlight the limiting value of the terminal temperature difference (TTD), below which the natural convection heat transfer becomes the sole heat transfer mode, i.e. the effect of surface radiation can be neglected. The effects of variations of emissivity and TTD are also presented.*

Nomenclature

c = Specific heat
c_r = Specific heat at reference temperature
c^* = Non-dimensional specific heat [$=c/c_r$]
F_{ij} = View factor of ith surface from jth surface
g = Acceleration due to gravity
Gr_r = Reference Grashoff number [$= g\beta_r (T_H–T_C)H /\nu_r$]
H = Cavity height
J = Radiosity
J^* = Non-dimensional radiosity [$=J/\sigma(T_H)^4$]
k = Thermal conductivity
k_r = Thermal conductivity at reference temperature
k^* = Non-dimensional thermal conductivity [$=k/k_r$]
N = Number of participating surfaces
Nh = Number of segments on hot wall
Nu = Nusselt number
p = Fluid pressure
p_r = Reference pressure
p^* = Non-dimensional pressure [$=p/p_r$]
Pr_r = Reference Prandtl number [$=\nu_r/\alpha_r$]
Q_T,Q_H = Total heat transfer at hot wall
Q_{conH} = Convective heat transfer at hot wall
Q_{conC} = Convective heat transfer at cold wall
Q_R,Q_{radH} = Radiative heat transfer at hot wall
Q_{radC} = Radiative heat transfer at cold wall
Q_C = Total heat transfer at cold wall
Q_N = Heat transfer in pure natural convection
$(Q_T–Q_N)/Q_N$ = Heat ratio
RC = Radiation-conduction parameter [$=H\sigma(T_H)^4/k_r(T_H–T_C)$]
Ra = Rayleigh number
T_H,T_C = Hot and cold wall temperature
TTD = Terminal temperature difference [$(T_H–T_C)$]
$(T_H–T_C)/T_C$ = Overheat ratio
T_r = Reference temperature
u,v = Fluid velocities
U,V = Non-dimensional fluid velocities
U_0 = Characteristic velocity [$=\sqrt{\{\beta_r gH(T_H–T_C)\}}$]

Greek symbols

β_r = Coefficient of volume expansion at reference temperature
θ = Non-dimensional temperature [$=(T–T_r)/(T_H–T_C)$]
ρ = Fluid density

International Journal of Numerical Methods for Heat & Fluid Flow, Vol. 9 No. 4, 1999, pp. 423-443.

ρ_r = Fluid density at reference temperature
ρ^* = Non-dimensional fluid density $[=\rho/\rho_r]$
μ = Fluid viscosity
μ_r = Fluid viscosity at reference temperature
μ^* = Non-dimensional fluid viscosity $[=\mu/\mu_r]$
σ = Stephan-Boltzman constant
ε_i = Emissivity of ith surface
α_r = Thermal diffusivity at reference temperature
ν_r = Kinematic viscosity at reference temperature

Introduction

The study of radiation, either combined with conduction or convection in multidimensional enclosure, has received significant attention in recent years due to its direct relevance in potential application areas. Since an exact analytical solution for most of these cases is impossible to achieve, need arises for development of some numerical tools to tackle such thermal problems. Not long ago, finite difference schemes were considered to be the only efficient numerical tool for solving steady, two dimensional natural convection equations. This is evident from the year of publication of a work by G. de Vahl Davis and I.P. Zones (1983) who have compared the results of other authors, on the study of natural convection in a differentially heated square cavity. These results were based on finite difference schemes. Basic assumptions associated with de Vahl Davis and Zones (1983) were very much simplified. Incorporation of Boussinesq approximation along with the striking simplifications like steady laminar flow of a Newtonian fluid were some of the salient features of de Vahl Davis and Zones (1983). Nevertheless, de Vahl Davis and Zones (1983) continued to be a widely referred work and enjoyed the distinction of being a "bench mark solution" over the following years. Since then, a number of changes have taken place. As far as the numerical method is concerned, researchers became increasingly interested with the use of finite element method for the solution of fluid dynamics and heat transfer problems. Like the finite difference formulation, several schemes are envisaged for the finite element method (FEM) too. From the point of view of application to FEM, the stream function-vorticity function approach was successfully employed by Stevens (1982), Baker (1973) and Cheng (1972). The complete stream function formulation using FEM has been reported by Olson (1973). Heinrich and Strata (1978) outlined the scheme for penalty finite element formulation. However, use of primitive variable approach is fast becoming popular although there are two major drawbacks.

First, the continuity is not exactly satisfied and second, one has to contend with large number of variables. However the compensating advantage is that the formulation is relatively simple and straightforward. As noted before, earlier investigations relied heavily on some simplifying assumptions. In subsequent developments, some of these assumptions were dispensed with. The first is associated with the universal adoption of Boussinesq approximation. It is generally known that this approximation is valid for small temperature difference. However, as thermal conditions become severe in some specialized application areas, it appeared that a more realistic approach will

result if the effect of variable property is taken into account. Polezahev (1967) seems to be an early investigator in this field. Some subsequent reports on problems involving variable property natural convection have been published by Macgregor and Emery (1969), Leonardi and Reizes (1979, 1981) and Fusegi and Farouk (1989). Zhong *et al.* (1985) addressed several important problems associated with variable property convection, like the reference temperature issue and the limits of Boussinesq approximation. They concluded that the Boussinesq approximation was generally valid when the overheat ratio is less than 0.1. The effect of variable properties on laminar free convection heat transfer of monoatomic gas, polyatomic gas, air and water has been reported by Shang and Wang (1990, 1991). They noted that for polyatomic gases the classical Boussinesq approximation did not hold good even for small ranges of overheat ratio.

Subsequent to these observations, it was soon realised that besides the variable property effect, the interaction of natural convection with radiation may have some significant role in thermal systems where a large overall temperature difference exists. In many natural convection processes, the radiative heat transfer may affect the temperature field and consequently the flow field through emission and absorption processes within the fluid. This effect may be negligibly small if the fluid is dry air. However, the emission of radiation by the boundaries may have an important bearing on the boundary temperatures. Because of the coupling between the thermal and flow fields through buoyancy effects, the changes in the boundary temperatures caused by the radiative transfer may exercise a stronger influence than expected.

However, in spite of its wide applications, the interaction analysis did not receive adequate attention. Larson and Viskanta (1976) appear to be early investigators who outlined the necessity of solving the coupled heat transfer problem involving both convection and radiation. Since then only a few case studies have been reported in which the combined heat transfer problem has been addressed. Larson (1981), Lloyd *et al.* (1979) and Chang *et al.* (1983) were some of the investigators who addressed this combined mode heat transfer problem. While most of these studies concentrated on different schemes for solving the radiation intensity equation, which is basically integro-differential in nature, surface radiation did not recieve much attention. Coupling of surface radiation with natural convection, has recently been described in the investigations of Sen and Sarkar (1995) and Akiyama and Chong (1997), where the effect of surface radiation on natural convection has been discussed in the light of changes in thermal and flow field in differentially heated square cavity. However, an important aspect does not appear to have been investigated, i.e. the effect of terminal temperature difference as far as the onset of effects of radiation is concerned. In this regard, emissivity of the bounding surfaces is also expected to exercise considerable influence. The present work therefore, in addition to focussing on the detail of the numerical method, also highlights some of the associated heat transfer aspects. Accordingly it is proposed to present the results of the present work in the following sequence:

- effect of variation of TTD;
- effect of variation surface emissivity; and
- associated heat transfer effect.

Governing equations and boundary conditions

For a steady, laminar, two-dimensional, variable property Newtonian fluid, the conservation equations may be expressed as follows:

$$\frac{\partial(\rho u)}{\partial x}+\frac{\partial(\rho v)}{\partial y}=0 \tag{1a}$$

$$\rho\left(u\frac{\partial u}{\partial x}+v\frac{\partial u}{\partial y}\right)=\frac{-\partial p}{\partial x}+\frac{\partial}{\partial x}\left[2\mu\frac{\partial u}{\partial x}-\frac{2\mu}{3}\left(\frac{\partial u}{\partial x}+\frac{\partial v}{\partial y}\right)\right]+\frac{\partial}{\partial y}\left[\mu\left(\frac{\partial u}{\partial y}+\frac{\partial v}{\partial x}\right)\right] \tag{1b}$$

$$\rho\left(u\frac{\partial v}{\partial x}+v\frac{\partial v}{\partial y}\right)=\frac{-\partial p}{\partial y}+\frac{\partial}{\partial y}\left[2\mu\frac{\partial v}{\partial y}-\frac{2\mu}{3}\left(\frac{\partial u}{\partial x}+\frac{\partial v}{\partial y}\right)\right]+\frac{\partial}{\partial x}\left[\mu\left(\frac{\partial u}{\partial y}+\frac{\partial v}{\partial x}\right)\right]-\rho g \tag{1c}$$

$$\frac{\partial}{\partial x}(\rho cuT)+\frac{\partial}{\partial y}(\rho cvT)=\frac{\partial}{\partial x}\left(k\frac{\partial T}{\partial x}\right)+\frac{\partial}{\partial y}\left(k\frac{\partial T}{\partial y}\right) \tag{1d}$$

In equation (1d), the effect of viscous dissipation and the work of compression has been neglected. Equations (1a-1d) are non- dimensionalised with the help of the following reference quantities: $X=x/H$; $Y=y/H$; $u_0=\sqrt{\{\beta_r gH(T_H-T_C)\}}$; $\rho^*=\rho/\rho_r$; $P^*=(p-p_r)/(\rho u_0^2)$; $\mu^*=\mu/\mu_0$; $c^*=c/c_r$; $k^*=k/k_r$; $Pr_r=\nu_r/\alpha_r$; $\theta=(T-T_r)/(T_H-T_C)$; $U=u/u_o$; $V=v/u_0$. Quantities with subscript "r" refer to the property values at the reference temperature. Throughout the present work, the cold wall temperature has been assumed to be the reference temperature. With the introduction of the above mentioned non-dimensional quantities into equations (1a-1d), one obtains the following system of equations:

$$\frac{\partial(\rho^* U)}{\partial X}+\frac{\partial(\rho^* V)}{\partial Y}=0 \tag{2a}$$

$$\begin{aligned}\rho^*\left(U\frac{\partial U}{\partial X}+V\frac{\partial U}{\partial Y}\right)=&\frac{-\partial P}{\partial X}+\frac{1}{\sqrt{Gr_r}}\frac{\partial}{\partial X}\left[2\mu^*\frac{\partial U}{\partial X}-\frac{2\mu^*}{3}\left(\frac{\partial U}{\partial X}+\frac{\partial V}{\partial Y}\right)\right]\\&+\frac{\partial}{\partial Y}\left[\mu^*\left(\frac{\partial U}{\partial Y}+\frac{\partial V}{\partial X}\right)\right]\frac{1}{\sqrt{Gr_r}}\end{aligned} \tag{2b}$$

$$\rho^*(\mathrm{U}\frac{\partial \mathrm{V}}{\partial \mathrm{X}} + \mathrm{V}\frac{\partial \mathrm{V}}{\partial \mathrm{Y}}) = \frac{-\partial \mathrm{P}}{\partial \mathrm{Y}} + \frac{1}{\sqrt{\mathrm{Gr_r}}}\frac{\partial}{\partial \mathrm{Y}}[2\mu^*\frac{\partial \mathrm{V}}{\partial \mathrm{Y}} - \frac{2\mu^*}{3}(\frac{\partial \mathrm{U}}{\partial \mathrm{X}} + \frac{\partial \mathrm{V}}{\partial \mathrm{Y}})] + \frac{\partial}{\partial X}[\mu^*(\frac{\partial U}{\partial Y} + \frac{\partial V}{\partial X})]\frac{1}{\sqrt{\mathrm{Gr_r}}} + \theta \quad (2c)$$

$$\frac{\partial}{\partial X}(\rho^* C^* U\theta) + \frac{\partial}{\partial Y}(\rho^* C^* V\theta) = \frac{1}{\mathrm{Pr_r}\sqrt{\mathrm{Gr_r}}}[\frac{\partial}{\partial X}(K^*\frac{\partial \theta}{\partial X}) + \frac{\partial}{\partial Y}(K^*\frac{\partial \theta}{\partial Y}) \quad (2d)$$

It may be noted that the body force term in equation (2c) is based on the difference between the local fluid density and the density corresponding to fluid hydrostatic equilibrium condition. Finally, the boundary conditions are described in Figure 1a. However, when surface radiation is to be considered the thermal boundary conditions at the insulated walls are modified as described below; as it has been assumed that the medium is not participating, the radiation phenomena will be limited to the boundary surfaces only. For pure convection cases, one substitutes, for adiabatic surfaces, $-\mathrm{k}(\partial \mathrm{T}/\partial \mathrm{Y}) = 0$. This needs to be slightly modified in the presence of surface radiation. The specification of boundary condition on the adiabatic surface is completed by equating the convective and radiative transfers on the plate as shown below:

$$-\mathrm{k}\frac{\partial \mathrm{T}}{\partial \mathrm{Y}}|_{\text{ ith surface}} = \mathrm{J_i} - \sum_{\mathrm{j}=1}^{\mathrm{N}} \mathrm{F_{ij}J_j}$$

Introducing non-dimensional quantities, the above boundary condition can be transformed in the following form:

$$\mathrm{k}^*\frac{\partial \theta}{\partial \mathrm{Y}} = \mathrm{RC}[\sum_{\mathrm{j}=1}^{\mathrm{N}} \mathrm{F_{ij}J_j^*} - \mathrm{J_i^*}] \quad (3)$$

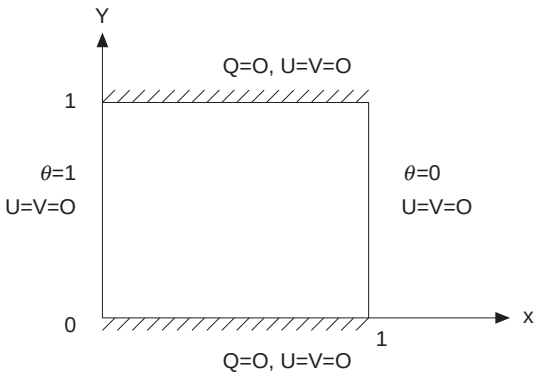

Figure 1a.
Test computational domain

where, $RC = [H\sigma(T_H)^4/k_r(T_H - T_C)]$ is the radiation-conduction parameter and $J^* = J/\sigma(T_H)^4$.

Equation (3) constitutes the gradient of the boundary condition for the energy equation (2d). Throughout the present work, the participating surfaces are assumed to be grey.

Finite element formulation and method of solution

Standard Galerkin formulation has been employed throughout the present work. However, some simplifying assumptions had to be made during the course of the discretization as illustrated below: for example, let us consider the discretization of (2d):

$$F_4 = \int N^T[\frac{\partial}{\partial X}(\rho^* c^* U\theta) + \frac{\partial}{\partial Y}(\rho^* c^* V\theta)]dA^{(e)} - \int \frac{1}{Pr_r\sqrt{Gr_r}} N^T[\frac{\partial}{\partial X}(k^* \frac{\partial\theta}{\partial X}) + \frac{\partial}{\partial Y}(k^* \frac{\partial\theta}{\partial Y})]dA^{(e)} \quad (4)$$

It has been assumed that the properties remain constant element wise. This assumption permits the negligence of the spatial variation of the property while computing the element stiffness matrix. So (2d) may recast as:

$$F_4 = \rho^{*(e)} c^{*(e)} \int N^T[\frac{\partial}{\partial X}(U\theta) + \frac{\partial}{\partial Y}(V\theta)]dA^{(e)} - \frac{k^{*(e)}}{Pr_r\sqrt{Gr_r}} \int N^T[(\frac{\partial^2\theta}{\partial X^2}) + (\frac{\partial^2\theta}{\partial Y^2})]dA^{(e)} \quad (5)$$

while computing the property values $\rho^{*(e)}$, $c^{*(e)}$, $k^{*(e)}$, $\mu^{*(e)}$, as the case may be, the temperature at the point ($\xi = \eta = 0$) is computed; subsequently, the property values are interpolated (corresponding to this temperature) from Ozisik (1985). The rest of the discretization scheme is analogous to the conventional methods of treating incompressible flow in which the non-linearities are treated by the Newton-Raphson method and the resulting simultaneous equations are solved by the Frontal solver. Detail of the methods are described elsewhere (Sarkar and Sastri, 1989). Convergence of the solution is assumed to be achieved when the largest residue is below a pre-assigned value, as low as 10^{-9} for pure convection cases. However, when radiation is present, this limit has to be raised to 10^{-8} due to slower convergence rate. During iterative process, (2a) to (2d) are solved first and the temperature distribution of the adiabatic surfaces are obtained. Subsequently, the following non-dimensional radiosity equations are

$$J_i^* - (1 - \varepsilon_i)\sum_{j=1}^{N} J_{ij}^* = \varepsilon_i(T_i/T_H)^4 \quad (6)$$

Where N denotes the number of discretized participating surfaces. For

isothermal surfaces, T_i assumes the values of T_H or T_C depending on its location. When the ith side corresponds to an adiabatic surface, the average temperature of that side of the element is considered.

A few words about the incorporation of radiative boundary condition i.e. equation (3) in the Galerkin formulation of the energy equation i.e. of equation (5) is in order. It may be noted that the radiative boundary condition involves only a differential of non-dimensional temperature with respect to the non-dimensional Y co-ordinate. So the term $(k^{*(e)}/Pr_r\sqrt{Gr_r})\int N^T(\partial\theta/\partial X)dY$ generated from the equation (6) can be neglected. Under the circumstances, after carrying out the integration of second order terms in equation (5), it takes the following form:

$$F_4 = \rho^{*(e)}c^{*(e)}\int N^T[\frac{\partial}{\partial X}(U\theta)+\frac{\partial}{\partial Y}(V\theta)]dA^{(e)}+\frac{1}{\sqrt{Gr_r}Pr_r}k^{*(e)}$$
$$[\int\frac{\partial N^T}{\partial Y}\frac{\partial\theta}{\partial Y}dA^{(e)}+\int\frac{\partial N^T}{\partial X}\frac{\partial\theta}{\partial X}dA^{(e)}]-\frac{k^{*(e)}}{Pr_r\sqrt{Gr_r}}\int N^T\frac{\partial\theta}{\partial Y}dX^{(e)} \quad (7)$$

From the structure of equation (7), it can be seen that a line integral along the domain boundary (i.e. the horizontal surfaces) appears in the last term which can accommodate equation (3) quite easily. So equation (7) may be finally recast in the following manner:

$$F_4 = \rho^{*(e)}c^{*(e)}\int N^T[\frac{\partial}{\partial X}(U\theta)+\frac{\partial}{\partial Y}(V\theta)]dA^{(e)}$$
$$+\frac{1}{Pr_r\sqrt{Gr_r}}k^{*(e)}[\int\frac{\partial N^T}{\partial Y}\frac{\partial\theta}{\partial Y}dA^{(e)}+\int\frac{\partial N^T}{\partial X}\frac{\partial\theta}{\partial X}dA^{(e)}] \quad (8)$$
$$-\frac{RC}{Pr_r\sqrt{Gr_r}}\int N^T[\sum_{j=1}^{N}F_{ij}J_j^*-J_i^*]dX^{(e)}$$

It may be noted that the last line integral in equation (8) needs to be evaluated only for these elements whose sides coincide with either of the horizontal surfaces. Since the last integral in equation (8) arises out of the interaction of conductive and radiative energy balances at the boundary, this can be treated as a source term during implementation of the Newton-Raphson scheme. Subsequent to the solution of (6), the Navier-Stokes and energy are solved once again; but this time (3) is considered as a boundary condition. The scheme is subsequently repeated. However, during two successive iterations the radiosity values are averaged. An initial attempt to use the current radiosity values directly during the subsequent iterations met with little success as far as the convergence of the scheme is concerned. This lack of convergence is more evident in connection with the present algorithm which employs the Newton-Raphson scheme.

It has been observed that the number of iterations are much more in the presence of radiation. For example, when pure convection is present, only six to seven iterations are necessary when one moves from Rayleigh number 10^5 to 10^6; whereas around 20 iterations are required under the same condition when radiation is present.

During the course of iteration the temperature of isothermal walls (T_H ,T_C) and emissivity has been supplied as the input. From the value of the cold wall temperature, the reference property values are obtained including the reference Prandtl number (Pr_r). For a specific Rayleigh number, the characteristic dimension of the cavity (H) may be calculated. From this value of the cavity dimension, the reference value of the velocity (U_0) can be calculated. The value of H is required in the computation of total energy transfer across the isothermal walls. The convective heat transfer from the hot wall can be calculated as:

$$Q_{conH} = -k_r H(T_H - T_C) \int_0^1 k^*(\partial\theta/\partial X)dY \tag{9}$$

and the radiative transfer for a segment i on the hot wall can be calculated as

$$q_{radH} = [J_i^* - \sum_{j=1}^{N} J_j^* F_{ij})\sigma(T_H)^4 \times \text{ (length of the element)} \tag{10}$$

So, the radiative transfer from the hot wall is

$$Q_{radH} = \sum_{i=1}^{Nh} q_{radH(i)} \tag{11}$$

Results and discussion

The FEM formulation as outlined above, has been used for generating a code and has been effectively employed in the present work for investigating the effect of surface radiation in a differentially heated square cavity. It may be noted that an eight noded isoparametric Taylor element has been used for the discretization of the computational domain.

Before a detailed discussion on the combined mode heat transfer can be initiated, a brief discussion on the grid independence study is necessary. In the present study, the mesh size is indicated by (M×N) in which M stands for the number of elements in X-direction and N for the same along Y-direction. The grid independence starts with a relatively coarse size mesh (14×14). The mesh in subsequent studies has been continuously refined up to a size of (26×14). The number of elements in the Y-direction had to be limited to 14, in order to restrain the size of the front width. Secondly it has been observed that the thermal gradients are predominantly along the X-direction at either of the

active walls. These lead to the fact that it is more demanding to increase the number of elements in X-direction than Y-direction. In the grid independence study, the effect of variable property convection and surface radiation has been considered. Table I shows the detail of such a study. During the study the value of cold wall temperature is kept constant at 300K, the hot wall temperature is assigned with 800K and emissivity is at 0.3. It is evident from the table that there is some disagreement of energy balances at active walls (less than 0.5 per cent) for all the grid sizes considered. This disagreement has also been reported in the published work (Leonardi and Riezes, 1981) for variable property natural convection. For the rest of the present work, computations have been performed on a 26×14 mesh.

Before detailed study of the results and their analysis, the validation of the present work for pure natural convection (i.e. $\varepsilon = 0$) is presented, due to nonavailability of published works in the area of present investigation. The variations of Nusselt number with Rayleigh number as obtained from the present work and that reported by Leonardi and Riezes (1981), for an over-heat ratio of 0.5, have been shown in the Figure 1b. It can be seen that the present work matches exactly up to $Ra=10^5$ while a little difference exists at $Ra=10^6$.

As can be seen from the nondimensional version of governing equations, there are four major parameters. These are the terminal temperature difference (i.e. TTD), surface emissivity and the parameters characterizing natural convection, i.e. Rayleigh number and the Prandtl number. As far as the

Grid	Q_{conH} (W)	Q_{radH} (W)	Q_H (W)	Q_{conC} (W)	Q_{radC} (W)	Q_C (W)
14×14	99.496	122.182	221.678	129.002	98.373	227.375
18×14	100.34	122.272	222.612	131.785	98.247	230.032
22×14	103.288	122.569	225.857	136.166	98.199	234.365
26×14	104.780	122.360	227.140	137.137	98.200	235.337

Notes: T_H =800K; T_C =300K; $Ra=10^6$; Pr_r =0.71; $\varepsilon = 0.3$

Table I.
Grid independence study for convection-radiation interaction

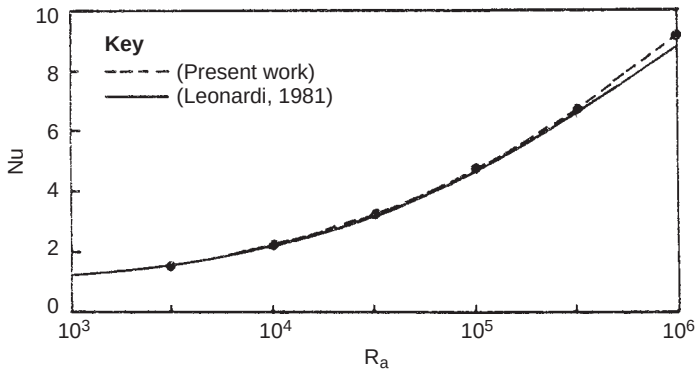

Figure 1b.
Variation of Nusselt number with Rayleigh number; $\varepsilon = 0, (\frac{T_H - T_C}{T_C} = 0.5)$

presentation of the results is concerned, the authors had to be selective in presenting the results in view of the large number of parameters involved. Consequently, the presentation is carried out in the following sequence.

Effect of variation of TTD

In this section, both the surface emissivity and Rayleigh number have been kept constant at 0.3 and 10^6 respectively. Figure 2 represents the development of thermal field as TTD is increased from 5K to 500K. Figure 2a represents the case with TTD=5K, which is characterized by the presence of a thermally statified core and near isothermal pools near the top and bottom horizontal boundaries. The crowding of isotherms at the bottom of the heated wall on the left and at the top of the cold wall on the right indicates the presence of strong convection in these regions. The near vertical nature of these isotherms, in these regions, amply demonstrates that the portion of the involved horizontal boundaries remain unaffected by either modes of heat transfer. The curvatures experienced by some typical isotherms at the bottom and top plates indicates that the gradients over there are governed by a combination of convection and radiation heat transfer modes (see equation (3)). As the TTD is increased to 300K, several important features of flow field are revealed (see Figure 2b). First, the isotherms near the heated plate have spread somewhat and the effect of radiation from the hot wall is more pronounced. Second, the size of the thermally stratified core has reduced somewhat. Also, the size of the isothermal pool at the top has increased in size while the one near the bottom horizontal boundary begun to lose its identity because of gradual intrusion of a number of isotherms into that region. The orientation also suggests that energy received by the bottom plate through radiation is conducted out i.e., the bottom plate is cooled by convection. Figure 2c represents the case when TTD is increased to 500K. The features, as described in connection with Figure 2b, are more pronounced now. The spreading of the isotherms near the heated plate is presumably due to a large increase in the value of thermal conductivity with change in temperature. For example, for a rise in temperature from 300K to 800K, the thermal conductivity increases by almost three times. Hence

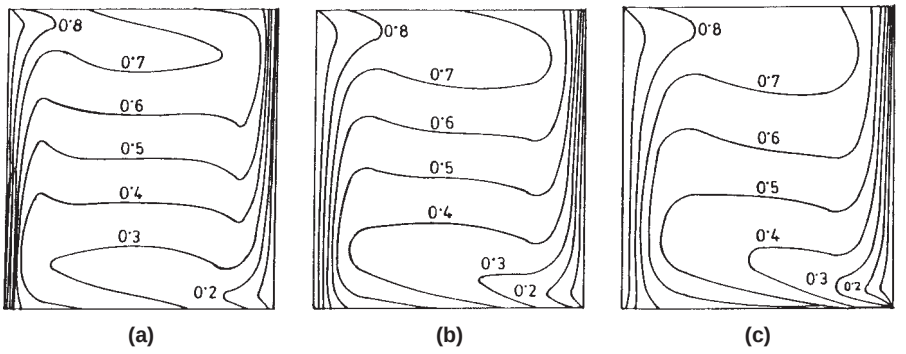

Figure 2.
Temperature distributions at $\varepsilon = 0.3$ and Ra = 10^6 for (a) TTD = 5K, (b) TTD = 300K, (c) TTD = 500K

although there is significant spreading of the isotherms, the convection heat transfer from the heated plate increases due to an increase in the value of thermal conductivity. Figure 2c reveals an interesting feature as far as the arrangement of isotherms near the bottom plate is concerned. It can be seen therefore that increase of TTD gradually leads to a situation in which a high temperature fluid layer can exist below a low temperature fluid layer. This leads to instability and often leads to convergence problems in numerical simulations involving still higher values of TTD. It is a kind of flow instability. It seems that this sort of instability is not apparently due to lack of discretization or drawback of finite element method. Figures 3a, 3b and 3c demonstrate the presence of not only thermally stratified cores as discussed earlier but also point to the fact that the cores are more or less stagnant too. The mid-plane vertical velocity distribution is shown in Figure 4. It is seen that as the TTD is increased, the maximum velocity in wall boundary layer is shifted away from the hot wall. Consequently, the boundary layer thickness also increases. The reason may be ascertained from the fact that with increase of hot wall temperature, the viscosity in its vicinity increases which lessens the possibility of occurrence of the maximum velocity close to the wall.

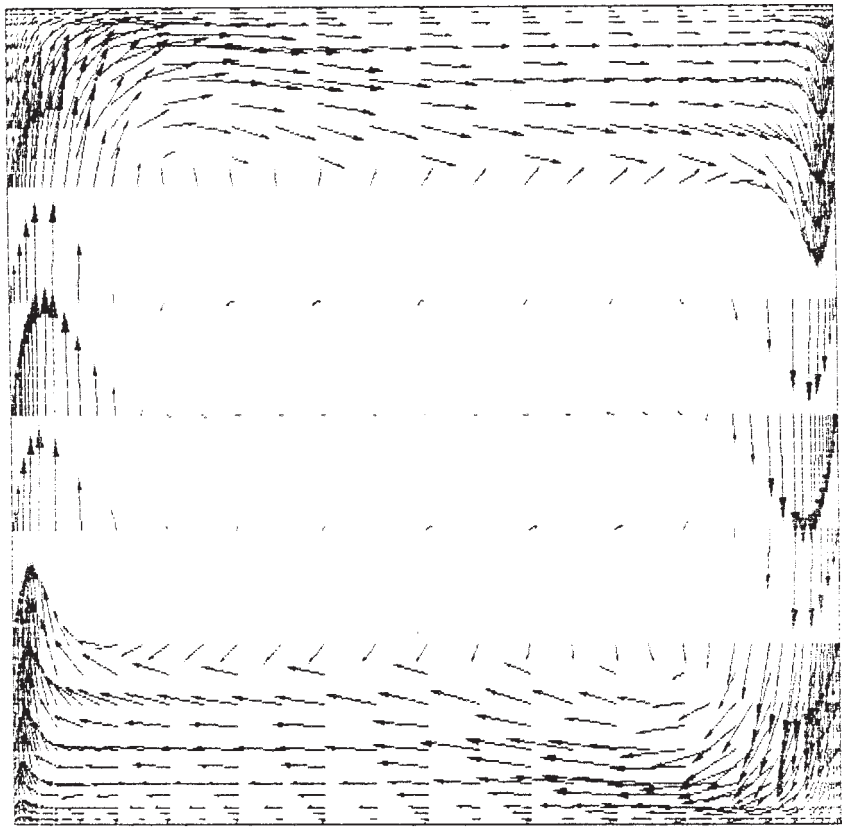

Figure 3a.
Velocity plot for $\varepsilon = 0.3$, TTD = 5K, Ra = 10^6

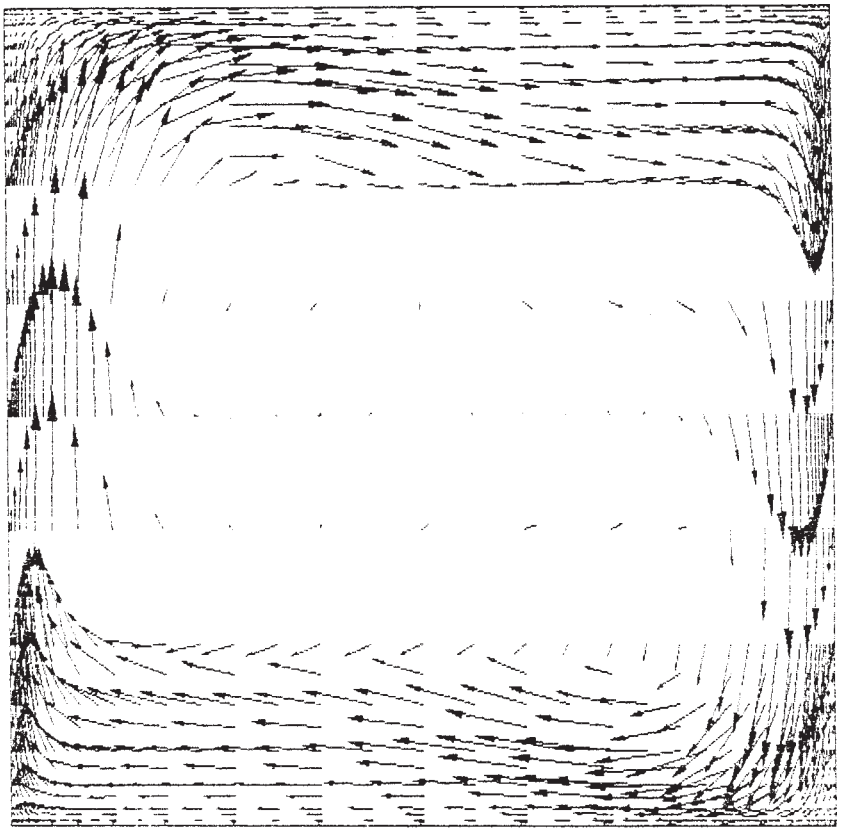

Figure 3b.
Velocity plot for $\varepsilon = 0.3$, TTD = 300K, Ra = 10^6

Effect of variation of surface emissivity

In this section, the value of TTD has been kept constant at 300K and the Rayleigh number is fixed at 10^6. Since the TTD has been kept constant, the variable property effect need not be considered at the hot wall. The first case with $\varepsilon = 0.0$ represents one in which the effect of surface radiation is neglected (see Figure 5a). As expected the core is stagnant and there appears to be two weak secondary vortices in the core region. Usually this flow is characterized by fast moving thin shear layers along the active vertical walls and horizontal jets along the insulated walls. When the surface emissivity is increased to 0.1 and 0.5 (see Figures 5b and 5c), no significant change in the flow structure is observed. This is expected in view of the constant values of TTD and the Rayleigh number. However, the associated thermal fields reveal some interesting aspects (see Figure 6). The isotherms near the heated wall have spread somewhat with increase of surface emissivity. This results in decrease of convective heat transfer. However the radiation heat transfer increases considerably due to increase in the value of the surface emissivity. It is also evident from the temperature distribution in the core that with increase in the value of emissivity, the core is more intensively heated. It is interesting to note

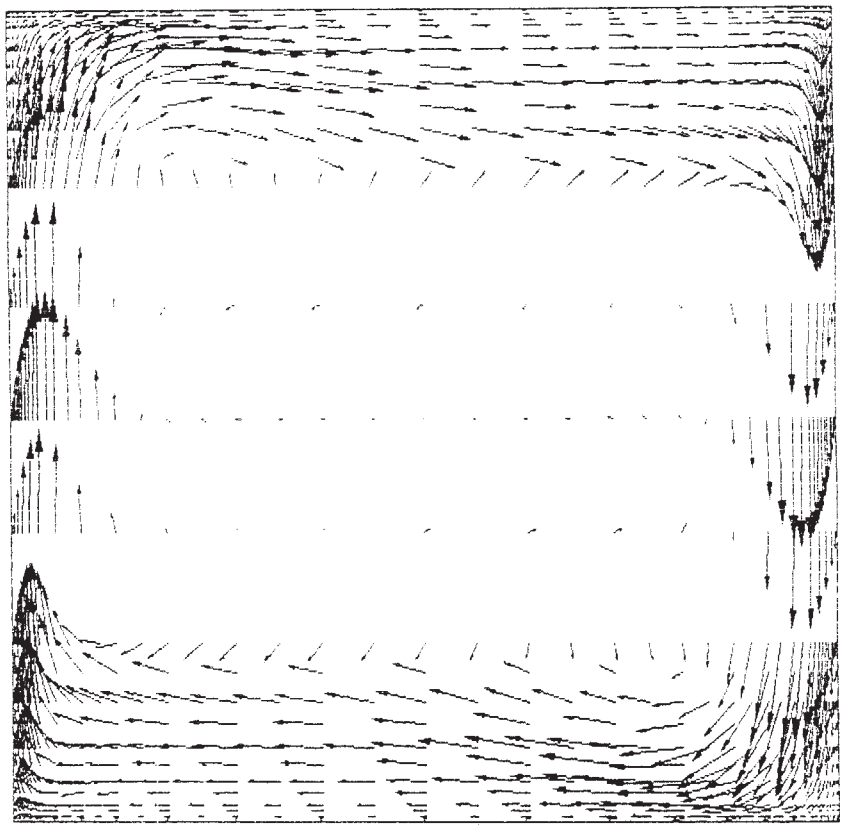

Figure 3c.
Velocity plot for $\varepsilon = 0.3$, TTD = 500K, Ra = 10^6

that with increase in emissivity the temperature of the upper horizontal plate decreases while the lower plate experiences the reverse trend. Figure 7 represents the heat flux distributions along the hot and cold wall. As can be

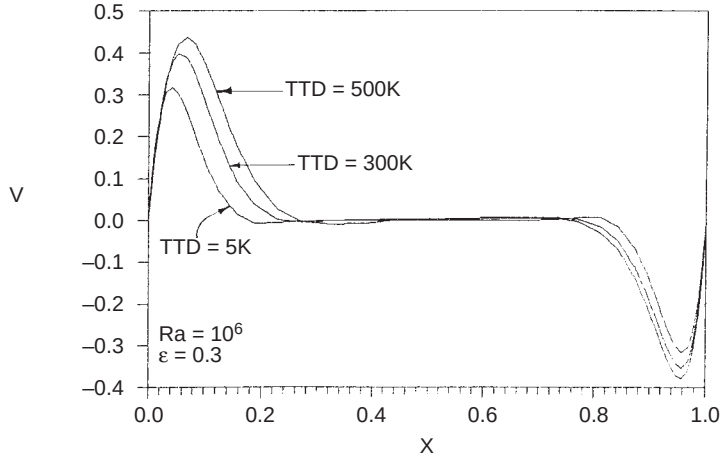

Figure 4.
Mid plane velocity distribution for different TTD

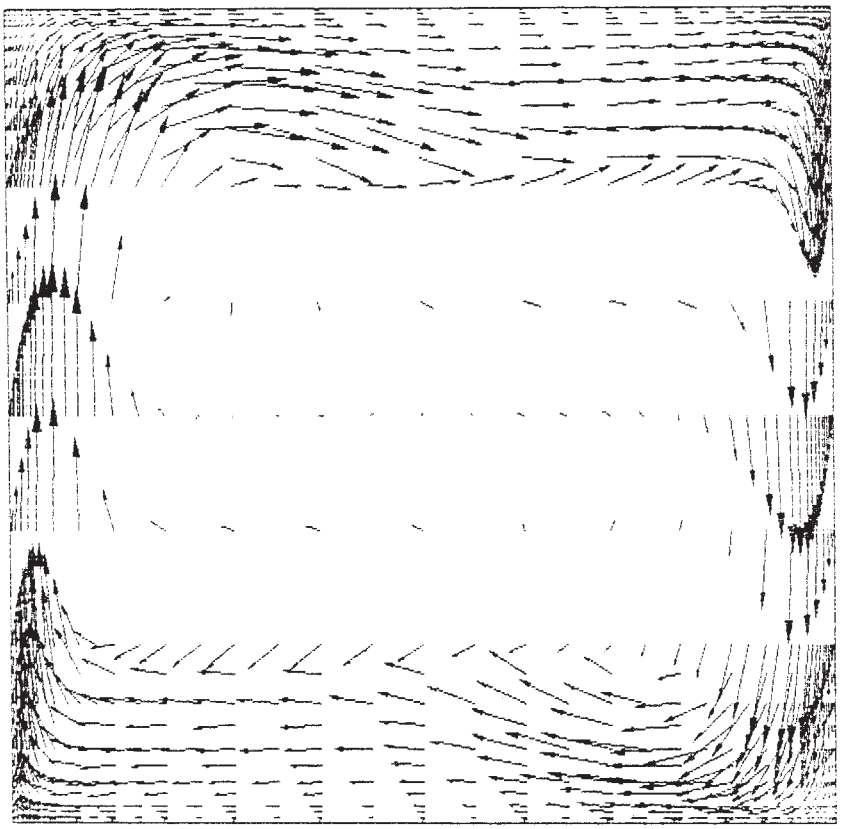

Figure 5a.
Velocity plot for $\varepsilon = 0$, TTD = 300K, Ra = 10^6

seen the patterns are typical of pure natural convection cases i.e., the heat flux is maximum for the cold wall, near the top while reverse is true for the heated plate. The areas under them indicate the amount of heat transfer from the respective walls. In Figure 7, heat flux distributions along the cold and hot wall are also shown for the cases with $\varepsilon = 0.1$ and $\varepsilon = 0.5$. In this case, the general observation is that the effect of increase of surface emissivity is to bring about a small variation in the heat flux distribution, be it cold wall or hot wall. It may be seen that the distribution of the energy transfer across either hot plate or cold plate has been discontinued near the corners. These corners, in fact, represent the singularities where there is sudden transition from insulated boundary condition to one of isothermal boundary condition. This means that although temperature continuity is ensured across the singularities, the gradients experience a discontinuity over there.

Heat transfer effects

In this section, an attempt will be made to highlight the heat transfer aspects for the problem under consideration. Figure 8 represents the variation of total heat transfer from hot wall keeping the value of Rayleigh Number constant at

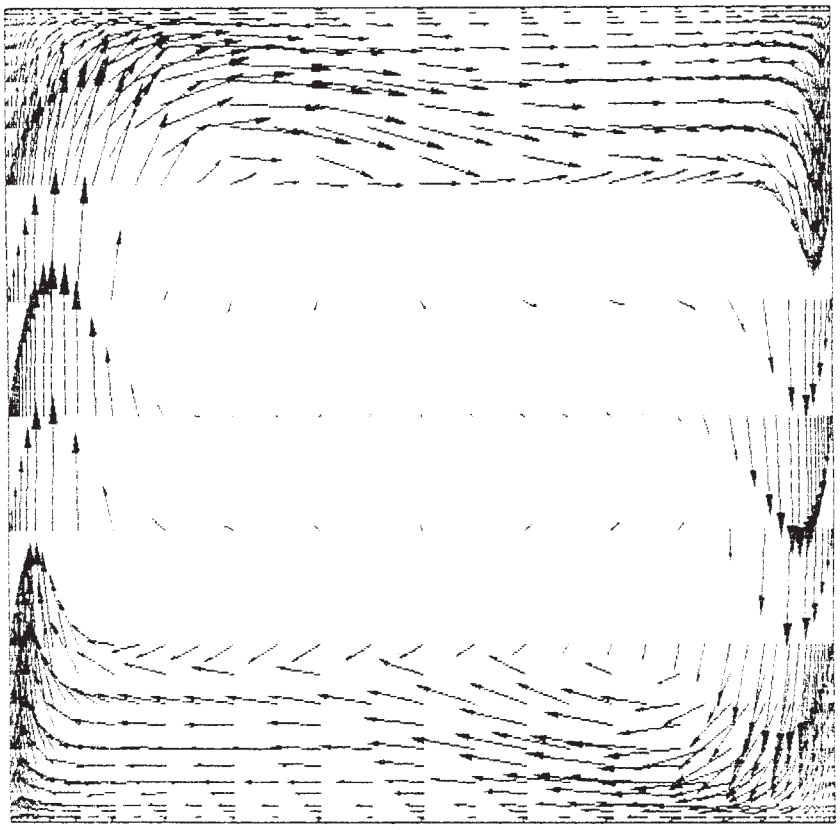

Figure 5b.
Velocity plot for $\varepsilon = 0.1$, TTD = 300K, Ra = 10^6

10^6 . The curve with $\varepsilon = 0$ represents the case of pure variable property natural convection. As expected, the convective heat transfer increases with increase of TTD; moreover the rate of increase of convective heat transfer over the range of TTD considered appears to be fairly constant. By rate it is implied that mention is made about the change of Q with respect to change of TTD. Now if a vertical line (see Figure 8) is drawn for a given value of TTD, the intercept for the $\varepsilon = 0$ curve will represent the value of Q_N while the remaining part of the intercept will be the additional increase of heat transfer over natural convection due to incorporation of radiation. Let us consider first the case with $\varepsilon = 0.1$. As can be seen, both Q_R and Q_N increases with TTD. However the rate of increase of Q_R is more than the rate of increase of Q_N. This is more pronounced as the value of ε is increased. For higher values of ε, the radiative heat transfer increases at a rapid rate as TTD increases. Figures 9a and 9b show the same aspects in a typical non-dimensional plane. The curve shows near the flat profile for a certain range of $(T_H - T_C)/T_C$ (over heat ratio) values whereafter Q_R/Q_N increases steadily. This means that within this region, the rates of increase of Q_R and Q_N are same. After this range, radiation contribution to heat transfer is much more pronounced i.e. consideration of natural convection alone may

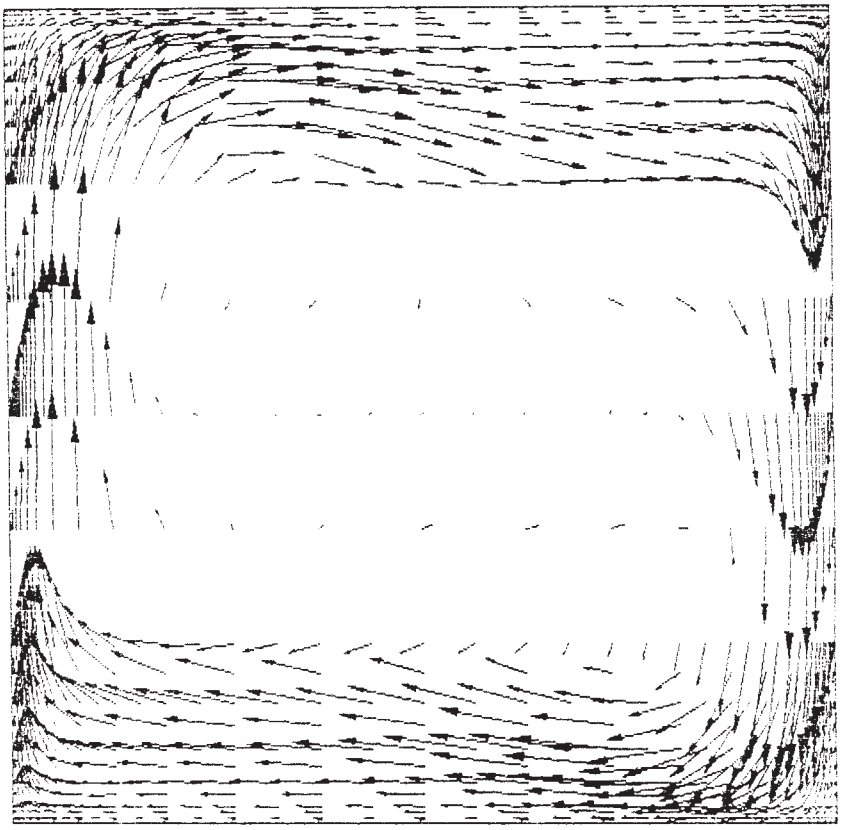

Figure 5c.
Velocity plot for $\varepsilon = 0.5$, TTD = 300K, Ra = 10^6

result in an underestimation of the heat transfer from the hot wall. Now let us consider the initial portion of the curve where Q_R/Q_N decreases with TTD. The drop in Q_R/Q_N with increase in TTD may be illustrated in the following manner:

$$Q_{conv} \text{ (hot wall)} = -K(TTD)(\partial\theta/\partial X)_{x=0} \quad (12)$$

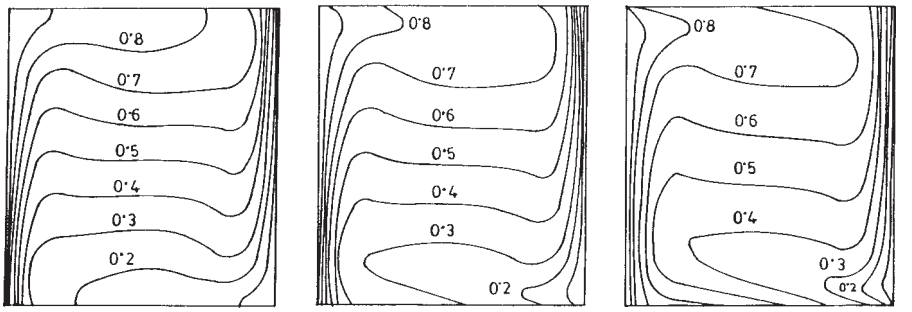

Figure 6.
Temperature distributions at Ra = 10^6 and TTD = 300K for ε = 0, 0.1, 0.5

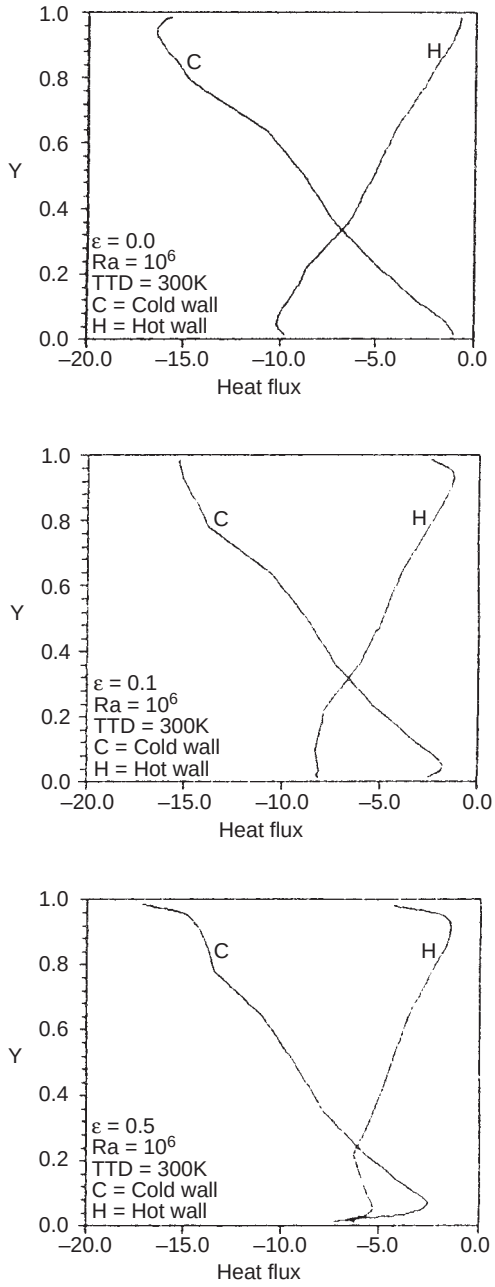

Figure 7.
Heat flux distribution along the cold and hot wall for ε = 0, 0.1, 0.5

For low values of TTD, the convective heat transfer from the hot wall is of the order of TTD, assuming negligible variation of K with TTD. So the rate of increase of heat transfer is constant and equal to the thermal conductivity at

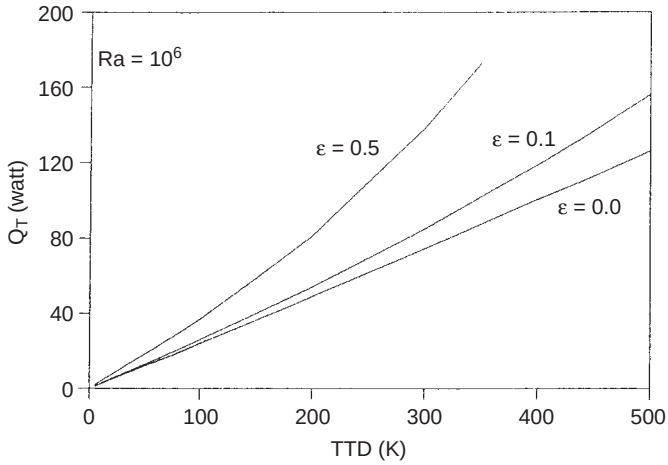

Figure 8.
Variation of total heat transfer with TTD and emissivity

the reference temperature. Now,

$$Q_R \cong 0[\sigma\varepsilon A.(TTD).(T_H + T_C)(\overset{2}{T}_H + \overset{2}{T}_C) \quad (13)$$

or,

$$Q/TTD \cong 0[\sigma\varepsilon H.(T_H + T_C)(T_H \overset{2}{+} T_C)^2 \quad (14)$$

Now let us consider the radiative transfer at two different values of TTD, with $T_C = 300K$, $Ra = 10^6$ and $\varepsilon = 0.1$

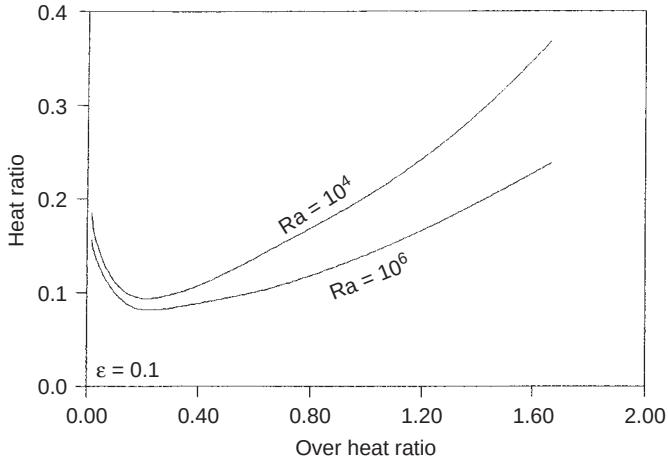

Figure 9a.
Variation of heat ratio with over heat ratio

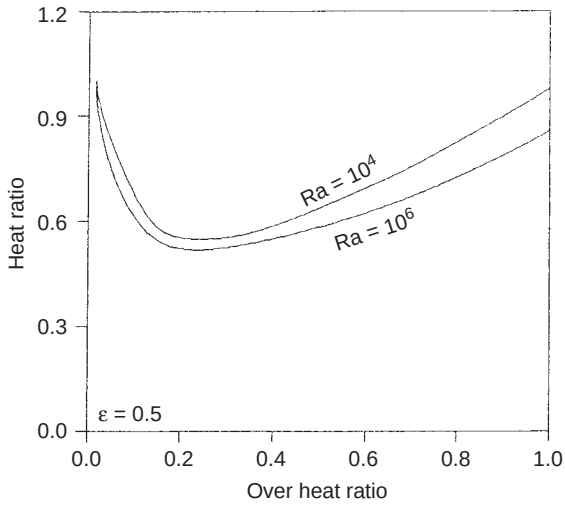

Figure 9b.
Variation of heat ratio with over heat ratio

$$\frac{[Q_R/TTD]_{TTD=350K}}{[Q_R/TTD]_{TTD=305K}} = \left[\frac{H_{350K}}{H_{305K}}\right]\left[\frac{(350+300)(350^2+300^2)}{(305+300)(305^2+300^2)}\right]$$
$$= (0.464)(1.25) = 0.58$$

In this calculation, the height of the cavity is determined from known values of Rayleigh number and TTD, while the property values are with respect to the reference temperature. What happens is that as TTD is increased (in the lower range), the height ratio goes on decreasing, while the other part goes on increasing. This increase is slow at the initial stages but develops rapidly in the upper ranges of TTD values, leaving a near flat zone in the lower range of TTD. Now if TTD is kept constant and Rayleigh number is increased the ordinate i.e. heat ratio will be lower since increased value of Ra results in stronger natural convection. Now let us consider the same sets of curves with different value of ε i.e. say $\varepsilon = 0.5$ (see Figure 9b). The nature of the curve remains the same. However there are some important points of difference too. Firstly these curves start with some higher values of heat ratio compared to the cases discussed in connection with Figure 9a. Since ε is higher, even at lower values of TTD, Q_R/Q_N will be higher. Secondly, the near flat zone has been shifted upwards. Also the zone occurs in the same range of TTD irrespective of the value of emissivity.

Conclusions

The present work shows in detail the numerical methodology of introducing surface radiation in the finite element formulation of variable property natural convection equations. The necessity of averaging radiosity in between two successive iterations values has also been outlined, since it leads to easier

convergence. From the point of view of heat transfer, there are a few interesting outcomes which are described below.

- The presence of radiation destroys the thermal stratification in the core and results in distribution of isotherms in such a manner as to lead to the instability in the thermal and flow field. This is one of the basic reasons behind non-convergence at higher values of Rayleigh Number and emissivity.
- It has been observed that when the reference temperature is 300K and the value of overheat ratio is around 0.35, radiation contribution to heat transfer starts to assume greater significance compared to its convective counterpart. It has also been observed that this value is independent of the Rayleigh Number and the surface emissivity.
- The trend in the variation of heat ratio with over heat ratio is similar for all values of emissivity.

References

Akiyama, M. and Chong, Q.P. (1997), "Numerical analysis of natural convection with surface radiation in a square enclosure", *Num. Heat Transfer*, Part A, Vol. 31, pp. 419-33.

Baker, A.J. (1973), "Finite element solution algorithm for viscous incompressible fluid dynamics", *Int. J. Num. Meth. in Eng.*, pp. 89-101.

Chang, L.C., Yang, K.T. and Lloyd, J.R. (1983), "Radiation natural convection interactions in two dimensional complex enclosures", *J. Heat Transfer*, Vol. 105, pp. 89-95.

Cheng, R.T. (1972), "Numerical solution of the Navier-Stokes equations by the finite element method", *Physics of Fluids*, pp. 2098-105.

de Vahl Davis, G. and Zones, I.P. (1983), "Natural convection in a square cavity: a comparison exercise", *Int. J. Num. Meth. in Fluids*, Vol. 3, pp. 227-48.

Fusegi, T. and Farouk, B. (1989), "Interaction analysis of natural convection and surface/gas radiation in a square cavity", *Proc. Num. Methods in Thermal Problems*, Vol. 6, Part I, pp. 588-99.

Heinrich, J.C. and Strata, N. (1978), "Penalty finite element analysis of natural convection at high Rayleigh numbers", *Finite Element in Fluids*, Vol. 4.

Larson, D.W. (1981), "Enclosed radiation and turbulent natural convection induced by fire", *Num. Meth. in Heat Transfer*, Wiley, New York, NY, pp. 467-87.

Larson, D.W. and Viskanta, R. (1976), "Transient combined laminar free convection and radiation in a rectangular enclosure", *J. Fluid Mech.*, Vol. 78, pp. 65-85.

Leonardi, E. and Reizes, J.A. (1979), "Natural convection in compressible fluids with variable properties", *Num. Meth. in Thermal Problems, Proc. of 1st Int. Conf.*, pp. 297-306.

Leonardi, E. and Reizes, J.A. (1981), "Convective flows in closed cavities with variable properties", in Lewis, R.W., Morgan, K. and Zienkiewicz, O.C. (Eds), *Num. Meth. in Heat Transfer*, John Wiley & Sons Ltd, pp. 387-412.

Lloyd, J.R., Yang, K.T. and Lin, V.K. (1979), "A numerical study of one dimensional surface, gas and soot radiation for turbulent bouyant flows in enclosures", *Proc. Natl Conf. Num. Meth. Heat Transfer*, pp. 142-61.

Macgregor, R.K. and Emery, A.F. (1969), "Free convection through vertical plane layers – moderate and high Prandtl number fluids", *J. Heat Transfer*, Vol. 91, pp. 391-403.

Olson, M.G. (1973), "Formulation of variational principle finite element method for viscous flow", *Proc. of the Conf. on the Variational Methods in Engineering*, Vol. 1.

Ozisik, M.N. (1985), *Heat Transfer, A Basic Approach*, McGraw-Hill, New York, NY.

Polezahev, V.I. (1967), "Numerical solution of a system of two dimensional unsteady Navier-Stokes equations for a compressible gas in a closed region", *Fluid Dynamics*, II, pp. 72-4.

Sarkar, A. and Sastri, V.M.K. (1989), "Finite element solution of steady,two dimensional, natural convection equations", *Proc. Num. Meth. Thermal Problems*, Vol. 2, Pineridge Press, Swansea, pp. 1732-42.

Sen, S. and Sarkar, A. (1995), "Effects of variable property and surface radiation on laminar natural convection in a square enclosure", *Int. J. Num. Meth. Heat Fluid Flow*, Vol. 5, pp. 615-27.

Shang, D.Y. and Wang, B.X. (1990), "Effect of variable thermo-physical properties on laminar free convection of gas", *Int. J. Heat and Mass Transfer*, Vol. 33, pp. 1387-95.

Shang, D.Y. and Wang, B.X. (1991), "Effect of variable thermo-physical properties on laminar free convection of polyatomic gas", *Int. J. Heat and Mass Transfer*, Vol. 34, pp. 749-55.

Stevens, W.N.R. (1982), "Finite element stream function – vorticity solution of steady laminar natural convection", *Int. J. Num. Meth. in Fluids*, pp. 349-66.

Zhong, Z.Y., Yang, K.T. and Lloyd, J.R. (1985), "Variable property effects in laminar natural convection in a square enclosure", *J. Heat Transfer*, Vol. 107, pp. 133-8.